Effect of the Axial Vibration of Screw on Total Shear Strain Distribution of Melt in Single-Screw Extruders

Yan-Hong Feng, Jin-Ping Qu, He-Zhi He, Bin Liu, Xian-Wu Cao, Sheng-Ping Wen

National Engineering Research Center of Novel Equipment for Polymer Processing, the Key Laboratory of Polymer Processing Engineering of Ministry of Education, South China University of Technology, Guangzhou 510641, China

Received 22 August 2006; accepted 3 November 2007
DOI 10.1002/app.27817
Published online 17 March 2008 in Wiley InterScience (www.interscience.wiley.com).

ABSTRACT: Single screw extruders are known as good melt pumps with the high, stable pressure needed for part extrusion. However they have a particular disadvantage in achieving good mixing. In a vibration-induced polymer extruder (VIPE), a vibration force field (VFF) is introduced into the whole extrusion process by the axial vibration of screw, which affects the mixing process. It is well-known that the total shear strain (TSS) has been widely used to measure the effect of melt mixing in a laminar system. In this study, an analytic model for pulsating TSS was developed and the TSS distribution of the melt in the screw channel of the melt conveying section in a VIPE was calculated to further understand the time-dependent dynamic laminar mixing process. A comparison of the TSS distribution of melt in screw channel with and without vibration shows that the TSS of melt increases with the application of vibration and the larger the vibration frequency and amplitude are, the larger the TSS that the melt may experience while melt traveling through the melt conveying section, which is favorable for melt mixing. © 2008 Wiley Periodicals, Inc. J Appl Polym Sci 108: 3917–3926, 2008

Key words: single-screw extruder; vibration-induced extrusion; total shear strain; mixing

INTRODUCTION

Single-screw extruders compared with twin-screw extruders have many advantages, such as lower costs, less maintenance and simpler operation. However, it has long been recognized that standard screws for plasticizing extruders are not efficient for mixing, so that single screw extruders are only well accepted in the compounding industry today for simple mixing operations.[1] Therefore, various mixing elements have been developed[2–4] to improve the mixing ability of single-screw extruders. Kwon et al. presented single-screw extruders with chaos screws which can enhance mixing process by the chaotic flow induced by spatially periodic barriers inserted in the screw channel.[5,6] Another noteworthy development is the BUSS Kneader. The construction and action of the Buss Kneader promotes a high degree of mixing. The screw continuously rotates and reciprocates or strokes; one full stroke for each revolution. Three rows of teeth are located on the circumference of the barrel at intervals of 120° and the flight of the screw is interrupted at appropriate points.[7]

As the mixing performance of a extruder considerably influences the quality and morphology of final products, the flow field in the mixing section has been studied by a number of authors to gain a better understanding of the process. However, studies on the mixing process show that the commonly used mixing elements are usually pressure consuming elements, and a general problem is that a good mixing ability of a mixing section always results in a decrease in throughput, increase in temperature and difficulty while cleaning.[1,8] On the other hand, starving feed was proposed to enhance the mixing capability of single-screw extruders, which also results in lower output.[9]

In a vibration-induced polymer extruder (VIPE)[10,11] presented in this work, a vibration exciter is connected with its screw, and a sinusoidal velocity in axial direction is superposed on the steady rotation of screw, thus the screw rotates pulsatingly with variable frequency and amplitude that can be changed conveniently according to the rheological properties of polymers, and the vibration force field (VFF) is applied to the entire extrusion process, as shown in Figure 1. This kind of vibration of screw is different from that of the BUSS reciprocating extruder of which the vibration frequency depends on the rotating speed of its screw. It has been proved by practice that, compared with

Correspondence to: Y. H. Feng (yhfeng@scut.edu.cn).
Contract grant sponsor: National Nature Science Foundation of China; contract grant numbers: 10472034, and 10590351.
Contract grant sponsor: Science and Technology Project of Guangzhou City; contract grant number: 2007Z2-D9151.

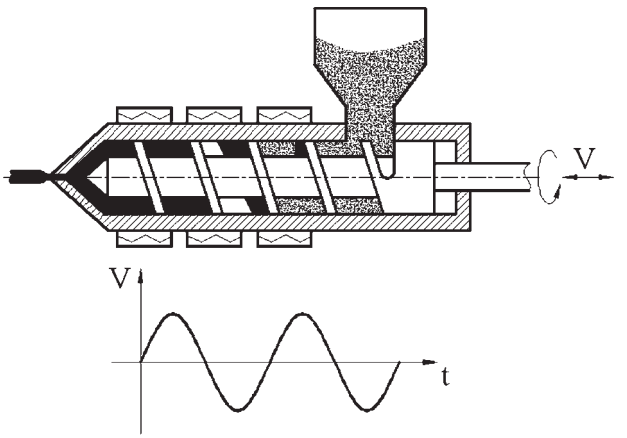

Figure 1 Diagrammatic sketch of VIPE.

the conventional single screw extruder, materials can be processed at lower average temperature with a VIPE, which means that a VIPE can lessen the temperature difference of melt and improve product qualities.[10,12]

To understand the distributive mixing in VIPEs, it is necessary to measure the degree of mixing. For regular flows, there are several mixing measures, such as: the decrease in striation thickness after the deformation of a stripe of finite thickness, the increase in interfacial area of two different materials after deformation, residence time distribution of materials, strain distribution and weighted average total strain, deformation characteristics and weighted average deformation characteristics.[13–15] In our previous work, the time-dependent residence time distribution in VIPEs has been discussed, which indicates that the application of vibration can lengthen the residence time of material.[16] In this study, the Total shear strain (TSS) distribution of melt in VIPEs was calculated to further understand the time-dependent dynamic laminar mixing process in VIPEs. The TSS may be used to measure the effect of melt mixing in a laminar system, such as the laminar mixing in a single-screw extruder. In a steady system, the magnitude of the TSS is governed by the shear rate and residence time. In extruders, both of the above factors are related to the initial position of fluid particle in screw channels. By calculating these two variables, the TSS distribution across screw channels may be solved.[13] Although the researches on the conventional TSS distribution have had great progress,[17,18] they can only describe the time-independent TSS distributions that are called steady TSS distributions and can not be used to describe the special time-dependent TSS distributions in VIPEs accurately. Therefore, the aim of the present work is to develop an analytic model for dynamic TSS distributions in VIPEs.

PULSATING TOTAL SHEAR STRAIN DISTRIBUTION

In a VIPE, the screw can not only rotate but also vibrate axially driven by a vibration exciter, as shown in Figure 1, thus, the steady melt conveying process becomes a periodically pulsating process. For the sake of simplification, the screw and barrel can be unrolled onto two planes, which is shown in Figure 2, the direction in the downstream direction is set to be z-direction, the direction perpendicular to the flight is set to be x-direction and the direction normal to the surface of the screw channel is set to be y-direction, thus the Cartesian coordinates can be established.

In the development of analyses for melt flow in the channels of single-screw extruders, the following assumptions are made: (1) The density of the melt is locally constant. (2) Chamfers or fillets on the flights may be neglected. (3) The depth and pitch of the screw channel are constant. (4) The ratio of the width of screw channel to the depth of screw channel is much larger than 10, namely, $W/H > 10$. (5) The influence of the flights is negligible, and there is no melt flow in the direction of channel depth. (6) There is no slip at the boundaries. (7) The temperature and thermal properties of melt keep unchanged. (8) The barrel rotates about a stationary screw.

Since the mixing quantity depends on the TSS γ that is the product of shear rate $\dot{\gamma}$ and residence time t, the distribution results of velocity and residence time of the melt in the melt conveying section with VFF are directly quoted from Ref. 16.

Velocity distribution

In Ref. 16, for the sake of simplification, dimensional analysis is applied, and the depth of the screw channel H, the cross-channel velocity component without vibration of the barrel v_x^0 and the downstream velocity component without vibration of the barrel v_z^0, period of axial vibration $T_0 = 2\pi/\omega$ and $p_0 = \eta_0 v_b^0/H$ are taken as characteristic quantities of length, velocity, time and pressure (stress), respectively, where ω is the angular frequency; $v_b^0 = \pi D\bar{N}$ is the relative velocity of the barrel to the screw, then $v_x^0 = \pi D\bar{N}\sin\theta = v_b^0\sin\theta$ and $v_z^0 = \pi D\bar{N}\cos\theta = v_b^0\cos\theta$, D is the external diameter

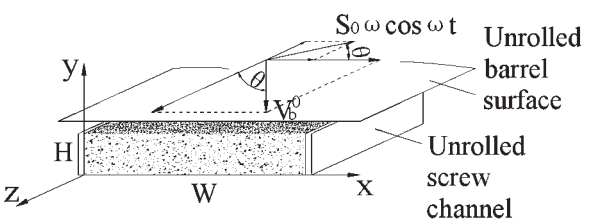

Figure 2 Schematic diagram of unrolled screw and barrel.

of screw, $\bar{N}$ is the average speed of rotation, θ is the helix angle, η_0 represents the apparent viscosity of melt with zero shear rate, and the following relationships are set: $v_x = v_x^0\tilde{v}_x$, $v_z = v_z^0\tilde{v}_z$, $p = p_0\tilde{p}$, $x = H\tilde{x}$, $y = H\tilde{y}$, $z = H\tilde{z}$, $t = T_0\tilde{t}$, where x, y, and z represent the coordinates in the cross channel direction, the depth direction and the downstream direction, respectively, t represents the time. For the sake of convenience, dimensionless marks $\sim$ are omitted in the following equations.

The dimensionless velocity components in the x and z directions are given as[16]

$$v_x = v_x(1)(2y - 3y^2) \tag{1}$$

$$v_z = v_z(1)[y + 3a(t)(y - y^2)] \tag{2}$$

where $v_x(1) = 1 + A_x\cos\omega t$, $v_z(1) = 1 + A_z\cos\omega t$ are the dimensionless pulsating velocity components in the x and z directions, respectively, at the dimensionless depth $y = 1$ which represents the barrel wall; $A_x = A\omega\cos\theta/v_x^0$ and $A_z = A\omega\sin\theta/v_z^0$ are the coefficients of vibration strength of the axial vibration in the x and z directions, respectively, where A is the amplitude of the axial vibration; $a(t) = Q_p(t)/Q_d(t) = 2\bar{Q}(1 + A_d\cos\omega t)/(1 + A_z\cos\omega t) - 1$ represents the instantaneous ratio of pressure flow to drag flow in the melt conveying section, $Q_d(t)$ is the drag flow rate, $Q_p(t)$ represents the pressure flow rate, $\bar{Q}$ is the time-averaged dimensionless volumetric flow rate, A_d is the amplitude coefficient of pulsating flow rate, and it can be proved that $A_d \approx A_z/\tan\theta = A_x\tan\theta$.[16] A special case is that when $A_z = 0$, and $A_d = 0$, namely, the steady extrusion without vibration, then, the ratio of pressure flow rate to drag flow rate of steady extrusion is

$$\frac{Q_p}{Q_d} = 2\bar{Q} - 1 \tag{3}$$

Setting $a = Q_p/Q_d$, then the dimensionless velocity in the z direction v_{zs} of steady extrusion can be given as

$$v_{zs} = v_z^0[y + 3a(y - y^2)] \tag{4}$$

Accordingly, the dimensionless velocity in the x direction v_{xs} of steady extrusion can be given as

$$v_{xs} = v_x^0(2y - 3y^2) \tag{5}$$

As shown in Figure 3, superposing the two components of v_z and v_x in the screw axial direction L, then the velocity in the axial direction of screw v_L is

$$v_L = v_z\sin\theta + v_x\cos\theta \tag{6}$$

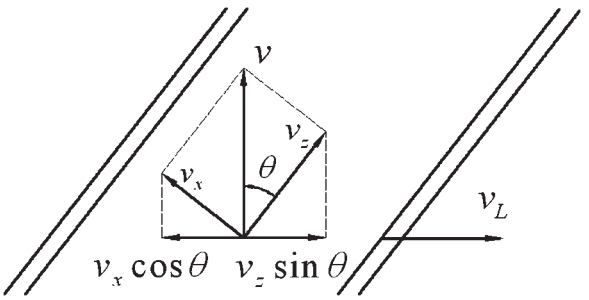

Figure 3 Velocity along the axial direction of screw.

Substituting eqs. (1) and (2) into eq. (6), then the expression of dimensionless velocity in the axial direction v_L is given as

$$v_L = 3y(1 - y)[1 + a(t)] + y\cos\omega t \times [A_z + 3A_z(1 - y)a(t) + 2A_x - 3A_xy] \tag{7}$$

Similarly, the dimensionless steady velocity in the axial direction v_{Ls} can be expressed as

$$v_{Ls} = 3y(1 - y)(1 + a) \tag{8}$$

Residence time distribution

It has been known that the flow rate in the x direction is zero, the transverse channel flow caused by v_x makes the material in screw channel roll over near the side of screw flight and form circulation flow.[16] Circulation flow can enhance the stirring and heat exchange, which is in favor of the homogenization of material and plays a key role of mixing. It can be deduced from eq. (1) that the melt flows around the dimensionless depth 2/3, thus the dimensionless depth 2/3 divides the screw channel into two parts in the depth direction. When $y > 2/3$, the direction of transverse channel flow is in the negative direction of x coordinate; and there exits a value of $y_c < 2/3$ corresponding to each value of y, and at this depth, the direction of transverse channel flow is in the positive direction of x coordinate, as shown in Figure 4, and satisfies

$$y = \left(\frac{1 - y_c}{2}\right)\left[1 + \left(\frac{1 + 3y_c}{1 - y_c}\right)^{0.5}\right] \tag{9}$$

$$y_c = \left(\frac{1 - y}{2}\right)\left[1 + \left(\frac{1 + 3y}{1 - y}\right)^{0.5}\right] \tag{10}$$

where $2/3 \le y \le 1$ and $0 \le y_c \le 2/3$.

Neglecting the time used for melt to flow in the y direction, then the dimensionless time used for a

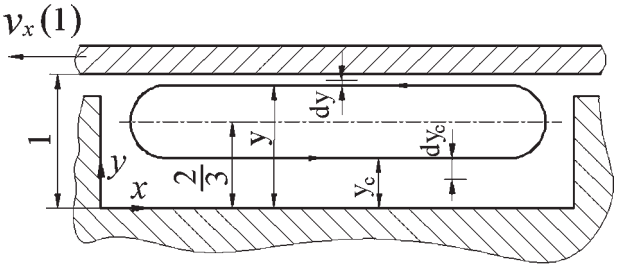

Figure 4 Circulation flow in the transverse channel direction in the screw channel.

particle flowing through a circulation can be defined as

$$t = \frac{W}{|v_x(y)|} + \frac{W}{|v_x(y_c)|} = t_1 + t_2 \tag{11}$$

where W is the dimensionless width of screw channel, t_1 and t_2 are dimensionless times for a particle flowing transversely through the upper and lower screw channel, respectively. Then the ratio of the time used for a particle flowing through the upper screw channel to the time used for a particle flowing through a whole circulation can be defined as

$$t_f = \frac{t_1}{t} = \frac{1}{1 + \left|\frac{v_x(y)}{v_x(y_c)}\right|} = \frac{1}{1 - \frac{y(2-3y)}{y_c(2-3y_c)}} \tag{12}$$

where $2/3 \le y \le 1$ and $0 \le y_c \le 2/3$.

Also taking the depth of screw channel H as characteristic length and setting the length of the melt conveying section of a screw $L = H\tilde{L}$, then omitting the dimensionless marks $\sim$, the dimensionless residence time of a particle in the melt conveying section of a typical screw is

$$t_L = \frac{L}{\overline{v_L}} \tag{13}$$

where $\overline{v_L}$ represents the dimensionless mean velocity in the axial direction of screw, obviously, it is a function of y

$$\overline{v_L} = v_L(y)t_f + v_L(y_c)(1 - t_f) \tag{14}$$

Substituting eqs. (14), (1), (10), and (7) into eq. (13), obtains

$$t_L = \frac{L}{6[1 + A_d \cos \omega t]\bar{Q}} \cdot \frac{\left[3y - 1 + 3\left(1 + 2y - 3y^2\right)^{0.5}\right]}{y\left[1 - y + \left[1 + 2y - 3y^2\right]^{0.5}\right]} \tag{15}$$

where $2/3 \le y \le 1$; or substituting eqs. (14), (1), (9), and (7) into eq. (13), obtains

$$t_L = \frac{L}{6(1 + A_d \cos \omega t)\bar{Q}} \cdot \frac{\left[3y_c - 1 + 3\left(1 + 2y_c - 3y_c^0\right)^{0.5}\right]}{y_c\left[1 - y_c + \left[1 + 2y_c - 3y_c^0\right]^{0.5}\right]} \tag{16}$$

where $0 \le y_c \le 2/3$.

Similarly, the dimensionless steady residence time t_{Ls} can be expressed as

$$t_{Ls} = \frac{L}{\overline{v_{Ls}}} = \frac{L \cdot (t_1 + t_2)}{v_{Ls}(y)t_1 + v_{Ls}(y_c)t_2} \tag{17}$$

Substituting eqs. (8), (5), and (10) into eq. (17), obtains

$$t_{Ls} = \frac{L}{6\bar{Q}} \cdot \frac{\left[3y - 1 + 3\left(1 + 2y - 3y^2\right)^{0.5}\right]}{y\left[1 - y + \left(1 + 2y - 3y^2\right)^{0.5}\right]} \tag{18}$$

where $2/3 \le y \le 1$; or substituting eqs. (8), (5), and (9) into eq. (17), obtains

$$t_{Ls} = \frac{L}{6\bar{Q}} \cdot \frac{\left[3y_c - 1 + 3\left(1 + 2y_c - 3y_c^2\right)^{0.5}\right]}{y_c\left[1 - y_c + \left(1 + 2y_c - 3y_c^2\right)^{0.5}\right]} \tag{19}$$

where $0 \le y_c \le 2/3$.

Total shear strain

The velocity components v_x and v_z, and the corresponding shear rate components $\dot{\gamma}_x$ and $\dot{\gamma}_z$ are different along the depth of screw channel. The mean shear rate components $\bar{\dot{\gamma}}_x$ and $\bar{\dot{\gamma}}_z$ are defined as the sum of time weighted shear rates at positions y and y_c[13]

$$\bar{\dot{\gamma}}_x = |\dot{\gamma}_x(y)|t_f + |\dot{\gamma}_x(y_c)|\left(1 - t_f\right) \tag{20}$$

$$\bar{\dot{\gamma}}_z = |\dot{\gamma}_z(y)|t_f + |\dot{\gamma}_z(y_c)|\left(1 - t_f\right) \tag{21}$$

where $0 \le y_c \le 2/3$, $2/3 \le y \le 1$. The dimensionless shear rate components $\dot{\gamma}_x$ and $\dot{\gamma}_z$ can be obtained by differentiating the corresponding dimensionless velocity components as

$$\dot{\gamma}_x = \frac{dv_x}{dy} = 2v_x(1)(1 - 3y) \tag{22}$$

$$\dot{\gamma}_z = \frac{dv_z}{dy} = v_z(1)[1 + 3a(t)(1 - 2y)] \tag{23}$$

Submitting eqs. (22) and (23) into eqs. (20) and (21), respectively, then the dimensionless mean shear

rate components in the x and z directions can be given as

$$\bar{\dot{\gamma}}_x = 2v_x(1)\left[(1-t_f)|1-3y_c| + t_f|1-3y|\right] \tag{24}$$

$$\bar{\dot{\gamma}}_z = v_z(1)[(1-t_f)|1+3a(t)-6y_c a(t)| + t_f|1+3a(t)-6ya(t)|] \tag{25}$$

The dimensionless TSS in the x and z directions can be given as

$$\gamma_x = \bar{\dot{\gamma}}_x t_L = \frac{2v_x(1)\cdot v_b^0 \sin\theta \cdot L}{v_b^0 \sin\theta\cos\theta \cdot 3[1+a(t)](1+A_z\cos\omega t)} \times \frac{(1-t_f)|1-3y_c| + t_f|1-3y|}{y(1-y)+t_f(y-y_c)(1-y-y_c)} = \frac{2L\cdot E(y)}{3[1+a(t)](1+A_z\cos\omega t)\cos\theta} \tag{26}$$

$$\gamma_z = \bar{\dot{\gamma}}_z t_L = \frac{v_z(1)\cdot v_b^0\cos\theta\cdot L}{v_b^0\sin\theta\cos\theta\cdot 3[1+a(t)](1+A_z\cos\omega t)} \times \frac{(1-t_f)|1+3a(t)-6y_c a(t)| + t_f|1+3a(t)-6ya(t)|}{y(1-y)+t_f(y-y_c)(1-y-y_c)} = \frac{L\cdot G(y,a(t))}{3[1+a(t)](1+A_z\cos\omega t)\sin\theta} \tag{27}$$

where

$$E(y) = \frac{(1-t_f)|1-3y_c| + t_f|1-3y|}{y_c(1-y_c)+t_f(y-y_c)(1-y-y_c)}$$

$$G(y,a(t)) = \frac{(1-t_f)|1+3a(t)-6ya(t)|}{y_c(1-y_c)+t_f(y-y_c)(1-y-y_c)} + \frac{t_f|1+3a(t)-6y_c a(t)|}{y_c(1-y_c)+t_f(y-y_c)(1-y-y_c)}$$

According to the definition of TSS presented by McKelvey,[19] the dimensionless pulsating TSS with vibration γ becomes

$$\gamma = \gamma_x + \gamma_z = \frac{L\cdot\left[\frac{2E(y)}{\cos\theta} + \frac{G(y,a(t))}{\sin\theta}\right]}{3[1+a(t)](1+A_z\cos\omega t)} \tag{28}$$

Similarly, with the corresponding steady velocity components and residence time, the components of the dimensionless steady TSS in the x and z directions can be obtained as

$$\gamma_{xs} = \bar{\dot{\gamma}}_{xs} t_L = \frac{2L\cdot E(y)}{3(1+a)\cos\theta} \tag{29}$$

$$\gamma_{zs} = \bar{\dot{\gamma}}_{zs} t_L = \frac{L\cdot G_s(y,a)}{3(1+a)\sin\theta} \tag{30}$$

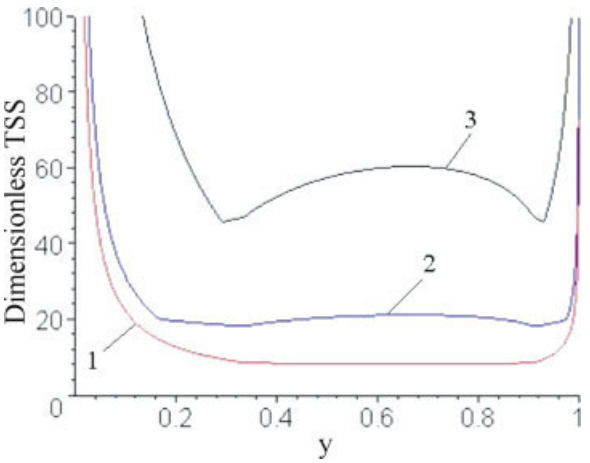

Figure 5 Curves of the dimensionless steady TSS distributions with different values of a; 1. $a = 0$; 2. $a = -0.5$; 3. $a = -0.8$. [Color figure can be viewed in the online issue, which is available at www.interscience.wiley.com.]

where $G_s(y,a) = [(1-t_f)|1+3a-6ya| + t_f|1+3a-6y_c a|]/[y_c(1-y_c)+t_f(y-y_c)(1-y-y_c)]$. Then the dimensionless steady TSS γ_s becomes

$$\gamma_s = \gamma_{xs} + \gamma_{zs} = \frac{L\cdot\left[\frac{2E(y)}{\cos\theta} + \frac{G_s(y,a)}{\sin\theta}\right]}{3(1+a)} \tag{31}$$

RESULTS AND DISCUSSION

According to eq. (31), the distribution of dimensionless steady TSS γ_s in the screw channel of the melt conveying section of a common single-screw has been obtained, as shown in Figure 5, where line 1 represents the pure drag flow. For the pure drag flow, the dimensionless TSS at $y = 2/3$ is the minimum, indicating the worst mixing effect. With the increase in head pressure, in other words, when there exits pressure flow Q_p, the dimensionless TSS increases, and there are two points of minimum dimensionless TSS, instead of one point at $y = 2/3$. These two points represent two depth positions that are called $y_{\min}$ and $y_{c\min}$, where $2/3 \le y_{\min} \le 1$ and $0 \le y_{c\min} \le 2/3$. On one hand, it represents that the particle flowing through the position $y_{\min}$ at the upper screw channel should also flow through the position $y_{c\min}$ at the lower screw channel; on the other hand, it represents that on the same cross channel section, the melt at these two positions experience the TSS of the same magnitude which is the minimum, just as shown in Figure 5. For a common screw extruder, if there is no mixing element at the melt conveying section, then the shear strain that material experiences would totally depend on the depth position of the material in the screw channel, and as long as the process conditions keep unchanged, the TSS distribution of the melt along the depth of screw channel would not change, which

results in the unchangeable difference of TSS of melt along the depth of screw channel, restraints the further improvement of mixing effect and influences the product qualities by property difference caused by the different shear strain experience of the material on the cross section of extrudates.

Figure 6 shows the dimensionless pulsating TSS distributions and the corresponding dimensionless steady TSS distribution obtained by eqs. (28) and (31), respectively. In Figure 6, the dimensionless average flow rates of Figure 6(a,b) are the same, while the vibration strength coefficient A_x of Figure 6(a) is larger than that of Figure 6(b); and the vibration strength coefficients of Figure 6(a,c) are the same, while the dimensionless average flow rate of Figure 6(a) is larger than that of Figure 6(c). As shown in Figure 6, upon the application of vibration, the dimensionless TSS varies periodically around the steady dimensionless TSS. A comparison of Figure 6(a,b) shows that the larger the vibration strength is, the larger the variation amplitude of dimensionless instantaneous TSS becomes. The comparison of Figure 6(a,c) shows that with the decrease in dimensionless average flow rate, namely with the increase in pressure flow, not only the dimensionless steady TSS will increase, the variation amplitude of dimensionless instantaneous TSS caused by the same vibration strength will increase too. In addition, it is also shown in Figure 6 that the positions of the minimum TSS of melt in the screw channel vary periodically during dynamic extrusion, which is quite different from the changeless dimensionless TSS distribution during steady extrusion. To illustrate the instantaneous movement of the position of the minimum TSS, the minimum point of dimensionless steady TSS A in Figure 6(c) is taken as an example. During a steady extrusion, melt flow through point A continuously, and the TSS of melt at this point will not change with time and always be the smallest. With the application of vibration, the TSS of the melt at point A will change periodically, sometimes it will become larger than the corresponding TSS at this point during steady extrusion, and sometimes it will become smaller than that during steady extrusion. During a vibration period, only at two moments, namely $(n+1/4)T$ and $(n+3/4)T$, where $n = 0, 1, 2, \ldots$, when the instantaneous TSS will be equal to the steady TSS at point A, thus during a vibration period the TSS at point A will not be the smallest except for the above two moments. On the cross section of a screw channel where point A exits, the position of the minimum instantaneous TSS of melt varies within a certain range, and the instantaneously change of TSS distribution is of great help to uniform the TSS at different position and hence improve mixing effect. It can also be observed that when keeping the average flow rate unchanged, the

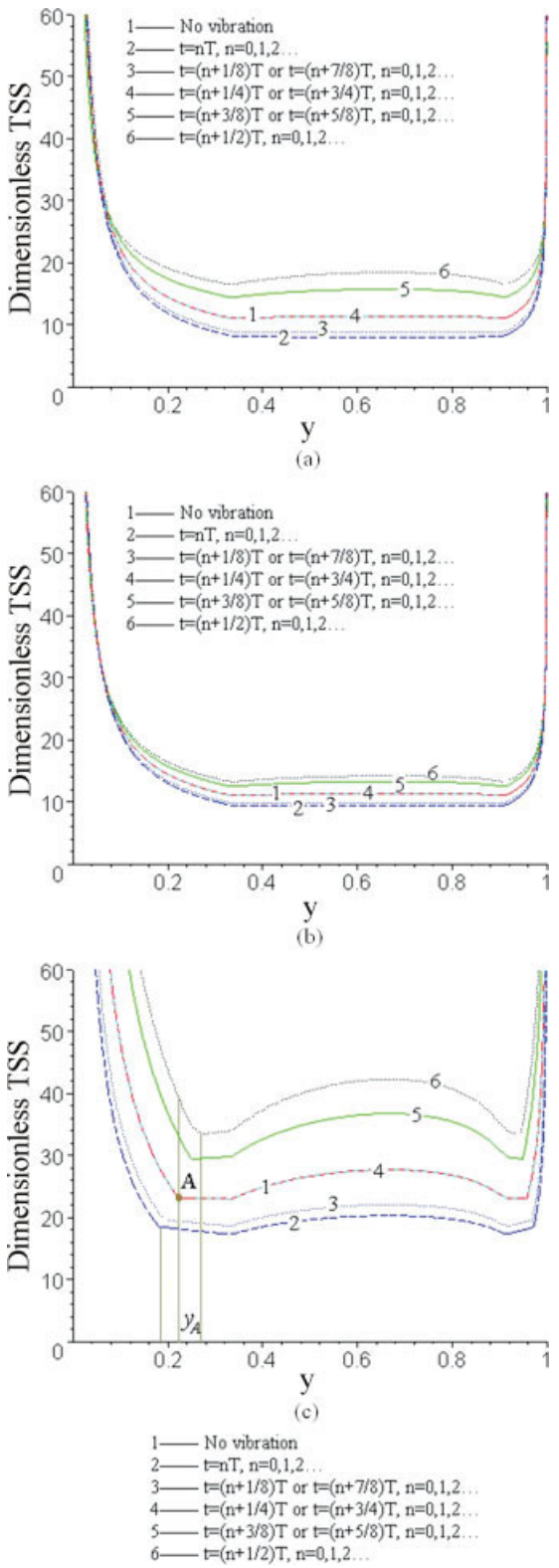

Figure 6 Dimensionless steady and pulsating TSS distributions (a) $A_x = 1$, $\bar{Q} = 0.4$; (b) $A_x = 0.5$, $\bar{Q} = 0.4$; (c) $A_x = 1$, $\bar{Q} = 0.2$. [Color figure can be viewed in the online issue, which is available at www.interscience.wiley.com.]

position of minimum instantaneous TSS changes within a larger range with the increase in vibration strength; and when keeping the vibration strength unchanged, the position of minimum instantaneous TSS changes within a larger range with the decrease in the average flow rate.

The above discussion investigated the influence of vibration on the pulsating TSS of melt in the screw channel from the instantaneous point of view. For a whole melt conveying and mixing process, the time-averaged pulsating TSS distribution must be solved. By time averaging eq. (28) over a vibration period, the time-averaged dimensionless pulsating TSS has been obtained. Figure 7 shows the time-averaged dimensionless pulsating TSS distribution and the corresponding dimensionless steady TSS distribution. It can be seen that the time-averaged dimensionless pulsating TSS is larger than the dimensionless steady TSS, which means that the application of vibration can improve the distributive mixing effect. It is worth noting that although there are also two points of the minimum TSS on the curve of the time-averaged pulsating TSS distribution, they are different from those on the curve of the steady TSS distribution. During a steady extrusion, the TSS of the melt flowing through those two minimum points is always the smallest, while during a dynamic extrusion, the instantaneous TSS of the melt flowing through those two time-averaged minimum points is not always the smallest.

Figure 8(a,b) show the curves of the periodic variation of the dimensionless pulsating TSS of melt at $y = 2/3$ with different vibration parameters. In Figure 8, the initial value of the coefficient of vibration strength in x-direction A_x is 0.5, and in Figure 8(a), the axial vibration frequency is fixed, and the axial vibration amplitude is enlarged two times greater; while in Figure 8(b), the axial vibration amplitude is fixed, and the axial vibration frequency is enlarged two times greater, both of the methods of changing the vibration parameters result in the same value of A_x, namely 1. It can be seen that, the instantaneous TSS varies periodically caused by the pulsating variation of the axial velocity, and compared with the corresponding steady TSS the maximum increment of the instantaneous TSS is larger than the maximum decrement of the instantaneous TSS. With the increase in vibration strength coefficient, the variation amplitude of the pulsating TSS increases, and the difference between the maximum increment and the maximum decrement of the TSS also increase.

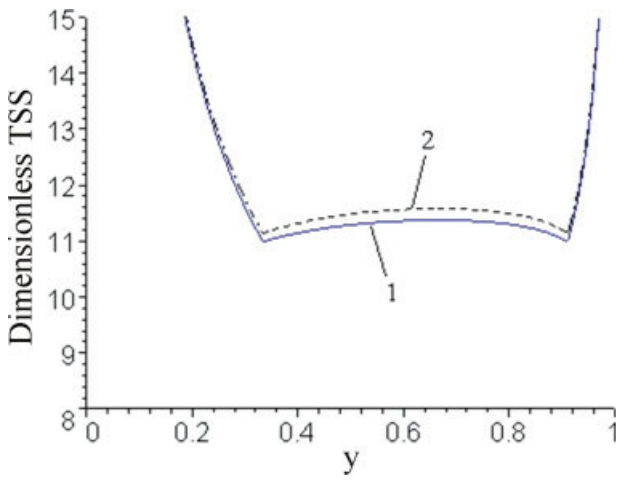

Figure 7 Dimensionless steady and time-averaged pulsating TSS distributions. 1. No vibration; 2. $A_x = 0.5$, $\bar{Q} = 0.4$. [Color figure can be viewed in the online issue, which is available at www.interscience.wiley.com.]

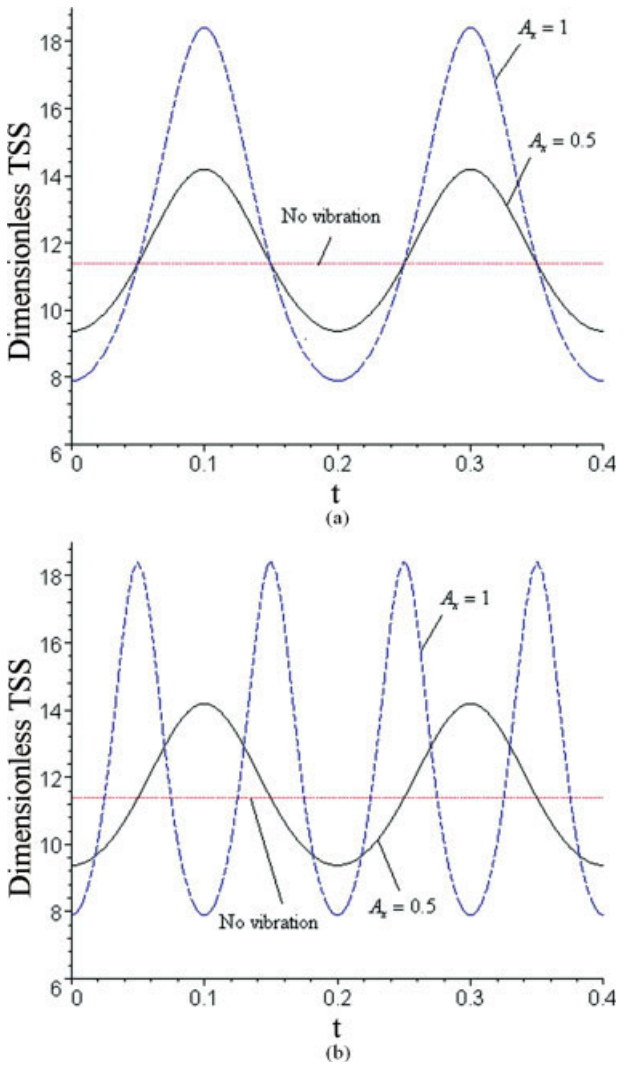

Figure 8 Curves of the periodic variation of the dimensionless transient TSS of melt at $y = 2/3$ with different vibration parameters; (a) amplitude varies while frequency fixed; (b) frequency varies while amplitude fixed. [Color figure can be viewed in the online issue, which is available at www.interscience.wiley.com.]

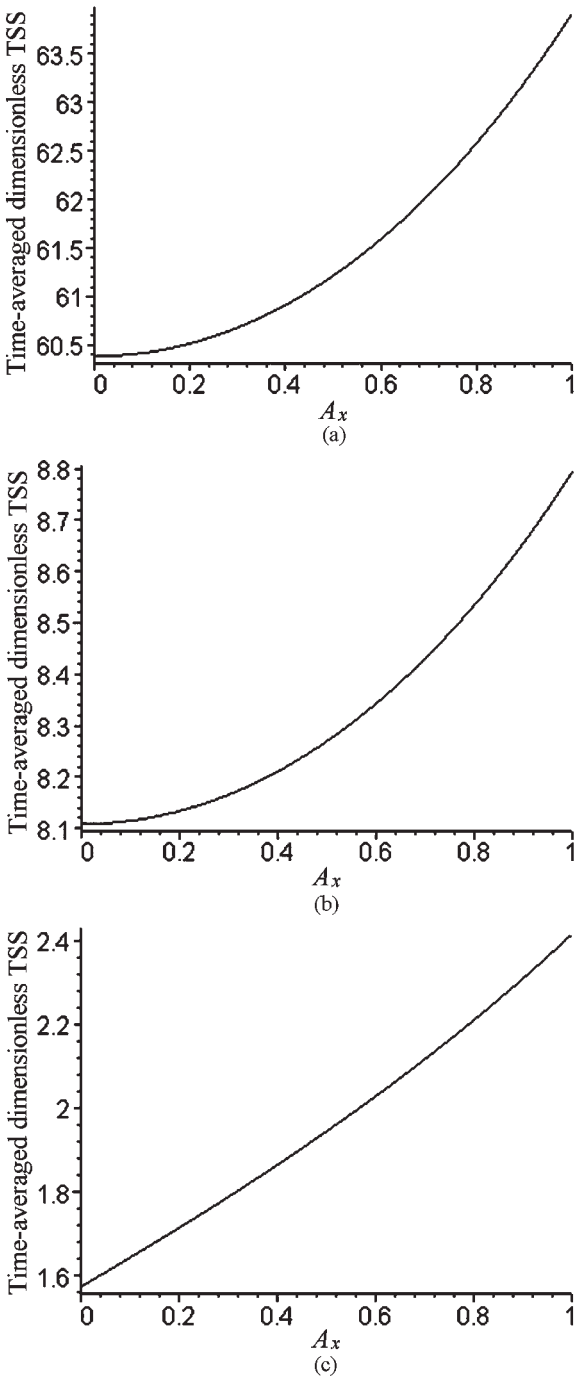

Figure 9 The graphs of the time-averaged dimensionless TSS against the coefficient of vibration strength at $y = 2/3$ with different dimensionless average flow rates (a) $\bar{Q} = 0.1$; (b) $\bar{Q} = 0.4$; (c) $\bar{Q} = 1$.

The positive and negative variation amplitudes are the same resulted from both of the methods of increasing the vibration strength, the difference is that when the axial vibration amplitude is kept unchanged and the frequency is increased, the variation times per unit time will increase.

Figure 9 shows the dependence of the time-averaged dimensionless pulsating TSS at $y = 2/3$ on vibration parameters, with different dimensionless average flow rates. It can be seen that, the lower the average flow rate is, the larger the time-averaged TSS becomes; with certain average flow rate, the time-averaged TSS increases with the increase in vibration strength coefficient, which indicates that the application of vibration helps increase the TSS and improves the mixing effect consequently; with the same vibration parameters, the lower the average flow rate is, the larger the increment of time-averaged TSS will be caused by vibration.

Figure 10 shows the dependence of the dimensionless steady TSS at $y = 2/3$ and the corresponding time-averaged dimensionless dynamic TSS with certain vibration parameters on the dimensionless flow rate, where line 1 represents the steady case. It can be seen that, both the dimensionless steady TSS and the corresponding time-averaged dimensionless dynamic TSS at $y = 2/3$ decrease with the increase in dimensionless flow rate; and due to the application of vibration, the time-averaged dimensionless dynamic TSS at $y = 2/3$ is always larger than the corresponding dimensionless steady TSS, which is favorable for melt mixing.

Figure 11 shows the curve of the increment rate of the time-averaged dynamic TSS of fixed vibration parameters to the steady TSS against average flow rate. It can be seen from Figure 9 that for certain vibration parameters, the increment of the time-averaged dimensionless TSS caused by vibration decreases with the increase in dimensionless average flow rate, however, because the dimensionless TSS decreases when the dimensionless flow rate

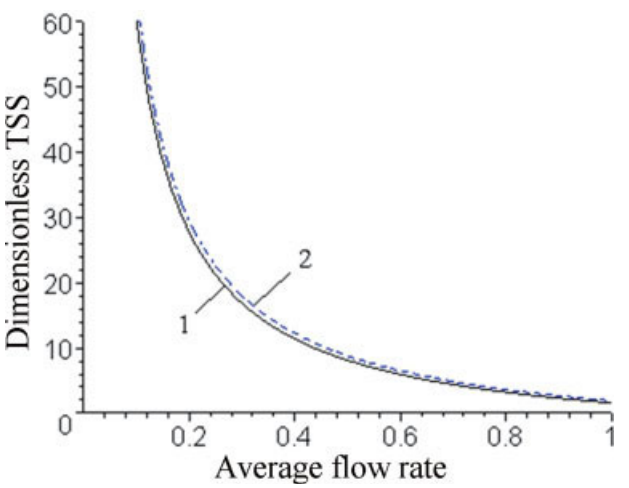

Figure 10 The graph of the dependence of the dimensionless TSS of melt at $y = 2/3$ without axial vibration and the corresponding time-averaged dimensionless TSS with certain vibration parameters on the dimensionless volumetric flow rate; 1. without vibration; 2. $A_x = 1$. [Color figure can be viewed in the online issue, which is available at www.interscience.wiley.com.]

increases, thus the increment rate of the time-averaged dimensionless TSS to that without vibration increases conversely with the increase in the dimensionless average flow rate. As it can be seen from Figure 5, larger flow rate will cause less TSS which indicates inferior mixing effect and restricts the increase in volumetric flow rate. The application of vibration can present larger increment rate for larger volumetric flow rate, which is an advantage of the vibration technology.

By averaging the time-averaged dynamic TSS and steady TSS over the whole depth of the screw channel, respectively, we obtained the means of the dynamic TSS and steady TSS. Figure 12 shows the curve of the increment rate of the mean of the dynamic TSS to that of steady TSS against the vibration parameters. It is worth noting that because of the assumption that there is no slip at the boundaries, the theoretical solution predicts that residence time of the melt at the barrel wall and screw channel surface would be infinite, thus the TSS of the melt would be infinite too, which is inconsistent with the actual conditions. In fact, the melt at these surfaces will keep interchanging position with adjacent melt and finally all the melt will leave the extruder. Thus, to obtain the dimensionless TSS over the whole depth of screw channel, the space interval of y is reduced to [0.1, 0.9]. It can be seen that compared with the steady TSS, with the same average flow rate, the increment rate of the TSS caused by the vibration is always positive, namely, the application of vibration can increase the mean TSS over the entire screw channel and improve the mixing effect. Moreover, the increment rate of the mean TSS increases with the increase in the coefficient of vibration strength, which indicates that the improvement

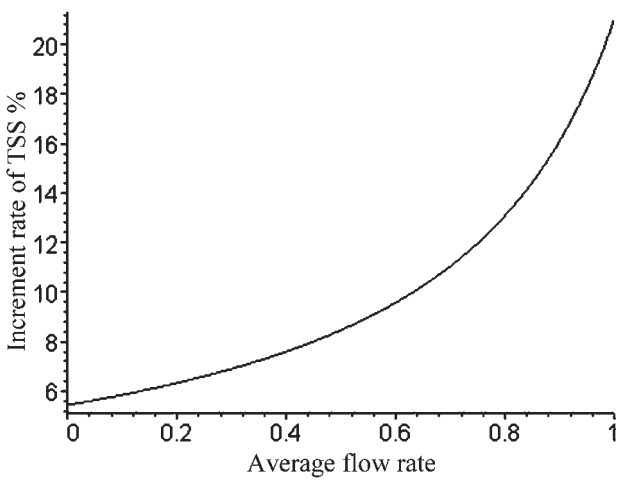

Figure 11 The relationship between the increment rate of the time-averaged dimensionless TSS of melt at $y = 2/3$ with vibration of fixed vibration parameters to that without vibration and the dimensionless average flow rate.

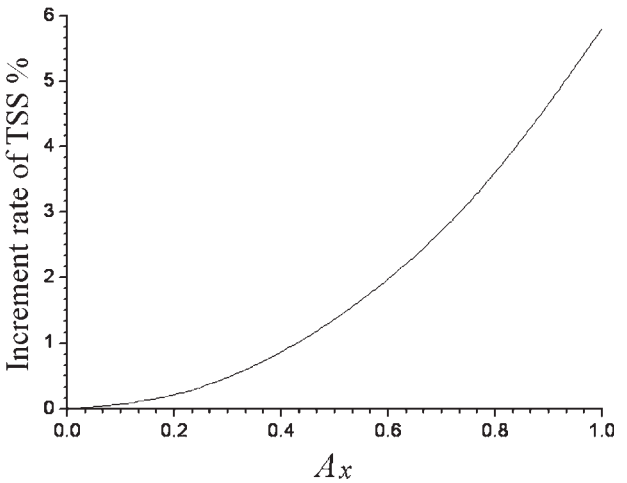

Figure 12 The graph of the increment rate of the time-averaged dimensionless TSS over the whole depth of screw channel with vibration to that without vibration against the vibration parameters with fixed dimensionless average flow rate.

of mixing effect caused by the application of VFF becomes more obvious with the increase in vibration strength.

CONCLUSIONS

In this study, the dimensionless pulsating TSS distribution of melt in the screw channel during the dynamic melt conveying was obtained. On the comparison of the dimensionless dynamic and steady TSS distributions, some general conclusions can be drawn.

1. Because of the application of axial vibration of screw, the TSS distribution of melt in the screw channel varies periodically, the period of the variation of TSS is the same as that of the velocity field, and the greater the vibration strength is, the larger the variation range of the transient TSS of melt becomes.
2. The time-averaged dynamic TSS increases compared with the steady TSS, which is favorable for melt mixing.
3. The position of the minimum point of the TSS in the screw channel changes instantaneously in a certain range after the application of VFF, which is in favor of homogenizing the shear strain course of melt at different position and improving mixing effect.
4. With the decrease in the average flow rate, the increment of the time-averaged dynamic TSS compared with the corresponding steady TSS increases even for the same vibration parameters.
5. With certain vibration parameters, the increment rate of time-averaged TSS increases with the increase in average flow rate.
6. Keeping the other conditions the same, the time-averaged TSS with vibration increases with the

increase in vibration frequency and amplitude, in other words, the increase in vibration strength can further increase the TSS of melt in the screw channel and improve the mixing effect.

In addition, the improvement of mixing ability caused by vibration is different from that caused by the mixing elements. The vibration parameters can be changed independent of other operating parameters especially rotary speed of screw. And it will not cause local high temperature and cleaning problems.

References

1. Gale, M. Adv Polym Technol 1997, 16, 251.
2. Plastics Additives and Compounding 1999, April/May, 30.
3. Plastics Additives and Compounding 2004, September/October, 50.
4. Yao, W. G.; Takahashi, K.; Koyama, K.; Dai, G. C. Polym Eng Sci 1997, 37, 615.
5. Hwang, W. R.; Kwon, T. H. Polym Eng Sci 2000, 40, 702.
6. Lee, T. H.; Kwon, T. H. Adv Polym Technol 1999, 18, 53.
7. Plastics Additives and Compounding 1999, July, 27.
8. Yao, W. G.; Takahashi, K.; Koyama, K.; Yamashita, Y. Polym Eng Sci 1998, 38, 1623.
9. Thompson, M. R.; Donoian, G.; Christiano, J. P. Polym Eng Sci 2000, 40, 2014.
10. Qu, J. P. J S. China University of Tech (Nat Sci) 1992, 20, 1.
11. Qu J. P. U. S. Patent 1993, 5,217,302.
12. Qu, J. P.; Xu, B. P.; Jin, G.; He, H. Z.; Peng, X. F. Plast Rubber Compos 2002, 31, 432.
13. Tadmor, Z.; Klein, I. Engineering Principles of Plasticating Extrusion; Krieger: New York, 1970.
14. Pinto, G.; Tadmor, Z. Polym Eng Sci 1970, 10, 279.
15. Tadmor, Z.; Gogos, C. Principles of Polymer Processing; Wiley: New York, 1979.
16. Qu, J. P.; Feng, Y. H.; He, H. Z.; Jin, G.; Cao, X. W. Polym Eng Sci 2006, 46, 198.
17. Kim, S. J.; Kwon, T. H. Polym Eng Sci 1996, 36, 1466.
18. Kim, S. J.; Kwon, T. H. Polym Eng Sci 1996, 36, 1454.
19. McKelvey, J. M. Polymer Processing; Wiley: New York, 1962.